Uluslararası İleri Doğa Bilimleri ve Mühendislik Araştırmaları Dergisi
Sayı 9, S. 27-38, 8, 2025

Araştırma Makalesi

IJANSER

https://as-proceeding.com/index.php/ijanser
ISSN:2980-0811

International Journal of Advanced Natural Sciences and Engineering Researches
Volume 9, pp. 27-38, 8, 2025

Research Article

Optimization of Laser Micromachining using Advanced Predictive Deep Learning

Aroosa Bibi* and Mamoona Khalid [2]

[1]*Department of Electrical Engineering, University of Engineering and Technology, Taxila, Pakistan*
[2] *Department of Electrical Engineering, University of Engineering and Technology, Taxila, Pakistan*

engineeraroosabibi@gmail.com

(Received: 26 July 2025, Accepted: 31 July 2025)

(3rd International Conference on Modern and Advanced Research ICMAR 2025, July 25-26, 2025)

ATIF/REFERENCE: Bibi, A. & Khalid, M. (2025). Optimization of Laser Micromachining using Advanced Predictive Deep Learning, *International Journal of Advanced Natural Sciences and Engineering Researches*, 9(8), 27-38.

Abstract – Ultrashort pulse laser micromachining is a transformative technology for precision manufacturing, enabling intricate microchannel fabrication across diverse applications such as semiconductors and microfluidics. This research presents a novel Deep Neural Network (DNN)-based simulator designed to autonomously predict optimal laser processing parameters, enhancing energy efficiency and precision. Implemented in Python within a Jupyter Note- book environment, the simulator leverages critical inputs, including microchannel dimensions, refractive index, optical absorption coefficient, and propagation loss, to optimize laser settings for materials like fluorides, germanates, and silicates. The model achieves high predictive accuracy, with R^2 scores exceeding 0.98 for pulse duration, repetition rate, and speed, and 0.93 for pulse energy, as validated through metrics like Mean Absolute Error (MAE) and Mean Squared Error (MSE). This work establishes a robust framework for automated parameter optimization, reducing experimental trials and advancing smart manufacturing. Future enhancements include real-time parameter adjustment and expanded material compatibility, positioning the simulator as a pivotal tool for industrial and academic applications.

Keywords – Ultrashort Pulse Laser Micromachining, DNN, MSE and MAE.

I. INTRODUCTION

Ultrashort pulse laser micromachining, utilizing pulses in the femtosecond to picosecond range, has revolutionized precision manufacturing by enabling high- quality microscale structuring with minimal thermal damage [1]. This technology is critical for applications in microfluidics, semiconductor devices, and biomedical engineering, where precise microchannel fabrication is essential. The process, particularly Femtosecond Laser Direct Writing (FLDW), allows for single- step, three-dimensional structuring with low propagation losses, making it ideal for advanced photonic systems [2].

However, optimizing laser parameters such as pulse duration, energy, repetition rate, and speed remains challenging due to material-specific optical and thermal properties. For instance, fluorides, germanates, and silicates exhibit dis- tinct refractive indices and absorption coefficients, necessitating tailored parameter adjustments [3]. Traditional optimization relies on time-intensive trial-and- error, which is inefficient and resource-heavy. Deep Neural Networks (DNNs) offer a solution by modeling complex, non-linear relationships in laser-material interactions, enabling automated parameter prediction [4].

This research develops a DNN-based simulator to predict optimal laser set- tings, enhancing precision and energy efficiency. By integrating material properties and microchannel dimensions, the simulator provides a scalable, automated approach to micromachining, addressing limitations in current manufacturing practices [5].

FLDW requires the manufacturing process of ultra-short pulses which enable interaction with pre-defined materials. The method lets operators guide both electron mobility and nuclear arrangement changes with precision. The stimulus for emission occurs through laser beam focusing and the machine generates photons using its gain medium [6]. A monochromatic beam from coherent photon emission creates interactions which can result in material ablation as well as melting or vaporization.

Ultrashort pulse laser micromachining employs sub-picosecond pulses to achieve precise material ablation with minimal heat-affected zones [6]. Its versatility enables processing of metals, ceramics, polymers, and biological tissues, supporting applications in microelectronics and biomedical engineering [7]. However, parameter optimization remains complex due to material variability and high equipment costs [8]. Predictive modeling enhances laser machining by optimizing parameters through machine learning and physical simulations. Neural networks and regression models predict outcomes based on historical data, reducing experimental costs [9]. Studies like Shimahara et al. (2023) demonstrate energy-efficient microchannel drilling using deep learning, though limited to specific materials [10]. Real- time error compensation, as explored by Mills et al. (2021), further improves efficiency [11].

DNNs excel in engineering applications by modeling complex, non-linear relationships. In laser machining, they predict parameters like pulse energy and speed based on material properties [4]. Applications span material science, energy systems, and robotics, where DNNs optimize processes and enable predictive maintenance [12]. Random Forest Regression, used in this study, is particularly effective for non-linear data due to its ensemble approach [13].

II. METHODOLOGY

Efficient laser parameter prediction for ultrashort pulse micromachining has been made possible by recent developments in machine learning. The model optimizes outputs like pulse duration, energy, repetition rate, and speed by using input factors like material type (fluoride, germanate, silicate), focal diameter, spatial dimensions, wavelength, propagation loss, refractive index, and optical absorption coefficient. A simplified block diagram of methodology is shown (see Figure 1). Developing the study project's strategy requires an effective combination of data preparation, DNN architecture design, and hyper parameter setting. Following are the respective steps for developing the simulator.

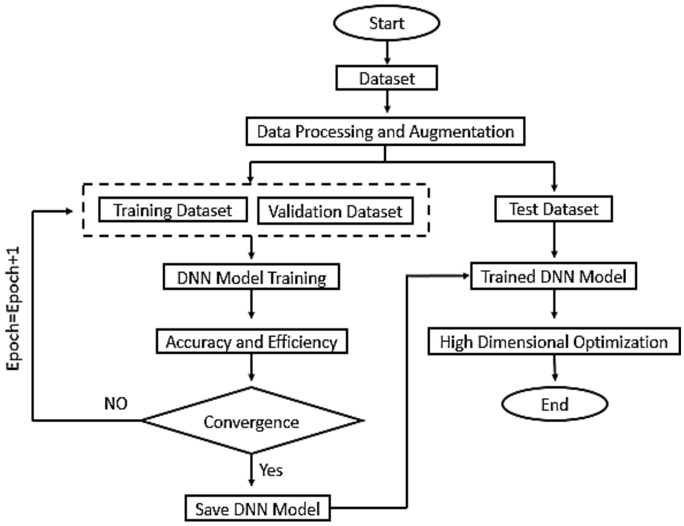

Fig 1: Proposed block diagram for the designing of DNN simulator.

A. *Dataset Preprocessing*

This study contains around 500 different sample examples that come from fluoride, germanate, and silicate materials. The research selected fifty laser micromachining examples with diverse material properties combined with various parameters for characterization. The system gathered various output results such as pulse duration together with pulse energy and repetition rate and machining speed under standardized experimental environments.

To ensure data integrity, multiple mathematically grounded techniques were applied:

1. Handling Missing Values For a feature vector $x = [x_1, x_2, \dots\dots.. x_n]$, if a value x_i is missing, we replace it using:
   Mean Imputation:
   $$x_i = \frac{1}{n}\sum_{j=1}^{n} x_{ij} \tag{1}$$
   where N is the number of non-missing samples.
   Median Imputation (if data is skewed):
   $$x_i = medium\ (x_{ij}) \tag{2}$$
2. Outlier removal was conducted using a two-step filter:
   Z-score filter:
   $$z = \frac{x_i - \mu}{\sigma} \tag{3}$$
   where μ is the mean of the feature, μ is the standard deviation and Values with $|z| > 3$ are considered outliers.

These steps ensured that noisy experimental anomalies were handled without losing valuable patterns in the data. The data required conversion before machines could process it effectively for learning purposes. This process made the model training faster while simultaneously enhancing the clarity of result interpretations. All features are normalized using Min-Max Normalization:

$$x_i^{norm} = \frac{x_i - \min(x)}{\max(x) - \min(x)} \tag{4}$$

This transformation rescales features to a 0–1 range, which helps in faster convergence of learning algorithms and avoids one feature dominating others due to its scale. The process of deriving significant parameter relationships made an essential part of feature engineering. For A combined parameter between maximum width and height was admitted into the model for data improvement as expressed;

$$D = \sqrt{(width)^2 - (height)^2} \tag{5}$$

The combined parameter represents dimensions of microchannels more accurately. Additional derived features, such as Deriving energy density values from experimental data allowed the dataset to gain contextually applicable information.

$$E_d = \frac{Pulse\ Energy\ (nJ)}{Focus\ Area\ (\mu m^2)} \tag{6}$$

where $Focus\ Area\ \pi(\frac{d}{2})^2$, by deriving these physical quantities like D and E_d, the model interpret data in terms that reflect true material behavior during machining. The performance assessment of the simulator required splitting the database into training and testing sections. Training of the DNN model involved approximately 80% of the evidence data which came from the training dataset. remaining 20% was reserved for testing.

B. *Data Preparation*

A standardization process transformed multiple input parameters which consist of focus diameter and depth in conjunction with wavelength as well as thermo-optic coefficient. Standardization and normalization techniques enabled the DNN model to work with parameters in consistent relative values thus avoiding dominant input features. For each input;

$$z = \frac{x_i - \mu}{\sigma} \tag{7}$$

where μ is the mean of the feature, μ is the standard deviation and Values with $|z| > 3$ are considered outliers.

$$x_i^{norm} = \frac{x_i - \min(x)}{\max(x) - \min(x)} \tag{8}$$

Standardization sets feature mean = 0 and variance = 1, making optimization gradients stable. Min-max normalization keeps the features within the [0,1] range. The researchers solved missing or incomplete data by implementing imputation techniques for all variables. Numerical parameters received mean or median substitutions during imputation but the mode served as the substitution value for categorical parameters. Identification of experimental outliers required the combination of interquartile range (IQR) with Z-scores statistical methods to process pulse energy and machining speed parameters.
Z-score filter:

$$z = \frac{x_i - \mu}{\sigma} \tag{9}$$

where μ is the mean of the feature, μ is the standard deviation and Values with $|z| > 3$ are considered outliers.
Interquartile Range (IQR):

$$IQR = Q_3 - Q_1 I \tag{10}$$

$$Outliers: x_i < Q_1 - 1.5 \times IQR\ or\ x_i > Q_3 + 1.5 \times IQR$$

These techniques identify extreme values that can distort learning. For example, a propagation loss of 1000 dB is unrealistic and will skew model weights if not removed.
This work contains mainly numerical parameters while converting any existing categorical features (such as material type) into machine-readable format. One-hot or label encoding methods enabled the preservation of data information before integrating models into the DNN framework. Categorical features like "Material Type" (fluoride, germanate, silicate) are converted to binary vectors so that the DNN can process them.

$$x_i = \begin{cases} 1 & if\ material\ = i \\ 0 & otherwise \end{cases} \tag{11}$$

Fluoride= [1,0,0], Germanate= [0,1,0] and Silicate= [0,0,1]
The model training benefited from scaling all input variable les to establish standardization across different parameter ranges. The dataset received min-max scaling as a normalization technique to harmonize the parameters of focus diameter (measured in micrometers) and propagation loss (measured in decibels). Smooth operations removed measurement noise and environmental noise detected in the collected dataset.

The model received evaluation through unbiased testing of training and validation and test subsets.

The data was separated into training (80%) and testing (20%) components that preserved data diversity within each segment. The methodology performed these preprocessing steps to develop a dataset which enabled effective training of the DNN-based simulator.

C. *Simulator Development*

Simulator development stands as the essential driver for improving ultrashort pulse laser micromachining methodology. Prediction and optimization of different laser machining procedures becomes possible through the processes of micromachining. parameters. In the context of your research, the development of a Deep Neural Network A DNN-based system acts as a reliable answer to the problems encountered during micromachining operations. The system combines both predictive and optimization functions through micromachining technology. The DNN design intentionally contains the following parameters shown in Table 1:

Table 1: Input and Output Parameters for Laser Micromachining

	Input Parameters	Output Parameters
1	Material	Pulse Duration (fs)
2	Focus Diameter(μm)	Pulse Energy (nJ)
3	Depth(μm)	Repetition Rate (kHz)
4	Max Width(μm) x Max Height(μm)	Speed (μm/s)
5	Wavelength(ns)	
6	Propagation Loss(dB)	
7	Refractive Index	
8	Thermo-Optic Coefficient	

The two fundamental optical characteristics of material-laser interaction determine propagation and light absorption through the refractive index (η) and optical absorption coefficient (α). The laser light needs to bend by a certain amount when entering into a substance which is quantified through the refractive index (η). It is calculated as;

$$\eta = \sqrt{\in_r \mu_r} \tag{12}$$

Where $\in_r$ is the relative permittivity the amount of material polarization within the field that how strongly the substance responds to electric field variations. and μ_r is the relative permeability by which a substance shows its reaction to the magnetic aspect within light. The minimum material spot size originates from the focus diameter (d_f) that relates beam waist (w_o) to laser wavelength (λ). It is given by:

$$d_f = \frac{4\lambda}{\pi w_o} \tag{13}$$

The specific measurement unit for laser wavelength is micrometers or nanometers where λ denotes the wavelength value. The narrowest point of the beam has a beam waist radius value designated as w_o. One pass of laser penetration or material removal is defined by the depth of ablation (d). Material ablation depth (d) depends on incident laser energy (E) and absorption coefficient (α) through the following calculation:

$$d = \frac{1}{\alpha} ln \frac{\mathrm{E}}{\mathrm{E}_{th}} \tag{14}$$

Where the laser pulse energy E serves as a measure in Joules to determine the applied quantity. Ablation beginning requires E_{th} threshold energy which stands for the minimum necessary energy. The optical absorption coefficient α measured in cm^{-1} determines light absorption strength of materials in terms of

cm^{-1} . The cross-sectional area of the microchannel (A) depends on its maximum properties of width (w) and height or depth (h) as measured during laser ablation.

$$A = w.h \tag{15}$$

According to research the wavelength of light has a significant impact on the minimal energy required to produce ablation. The threshold energy shows an inverse relationship with the square of wavelength values.

$$E_{th} \propto \frac{1}{\lambda^2} \tag{16}$$

This mean lower wavelengths reduce the power needed to start material removal which enables exact micromachining operations. Thermo-optic coefficient (β) measures the alteration of material refractive index when temperature shifts (ΔT). The calculation for refractive index modification depends on the following equation:

$$\Delta n = \beta \Delta T \tag{17}$$

Where the thermo-optic coefficient β exists as a measurement unit per °C. The temperature variation expressed in degrees Celsius takes the symbol ΔT. The capability of a material to predict laser heating effects during machining makes this property essential. The pulse duration (τ) refers to the time over which the laser emits energy in a single pulse. The formula connects pulse energy quantity (E) with peak power value (P_o).

$$\tau = \frac{E}{P_o} \tag{18}$$

Where the pulse energy E has units of Joules and the peak power of the pulse equals P_o. while measurement unit remains in Watts. The pulse energy (E) calculates using average power output (P_{avg}) and repetition rate (f) according to the following equation:

$$E = \frac{P_{avg}}{f} \tag{19}$$

where P_{avg} is average power and f is repetition rate. The repetition rate (f) affects the degree of pulse overlap during laser scanning. The overlap ratio (O) is expressed as:

$$O = \frac{v}{f.d_f} \tag{20}$$

where v is the scanning speed (μm/s or mm/s) and df is the focus diameter (μm). Higher overlap means that consecutive laser pulses hit closer areas, affecting the smoothness and depth of the machined channel. Material removal rate (R) is affected by multiplying scanning speed (v) with the channel cross-sectional area (A);

$$R = v.A \tag{21}$$

where the material removal rate (R) in μm^3 /s results from multiplication of the scanning speed (v) by the microchannel cross-sectional area (A).

III. RESULTS

The research investigates evaluation results obtained from using a DNN-based simulator to forecast laser micromachining parameters. The predictor evaluated its forecasting ability through measurements across all material types combined with different microchannel configurations. The simulator needed to identify its capability for accurate representation of experimental laser processing results including pulse duration, pulse energy, repetition rate and machining speed values. Different sample cases provided input for both experimental and simulated data comparison to evaluate prediction accuracy.

One of the fluoride samples was evaluated and compared our predicted simulator's performance to the actual experimental results. Variations between real and anticipated values were modest (see Figure 2). The error margin was remarkably modest, with pulse duration deviating by only 0.32%, pulse energy by 0.94%, repetition rate by 0.17%, and speed by 0.16%. This precision highlights the efficiency of our simulator in forecasting the best laser processing parameters.

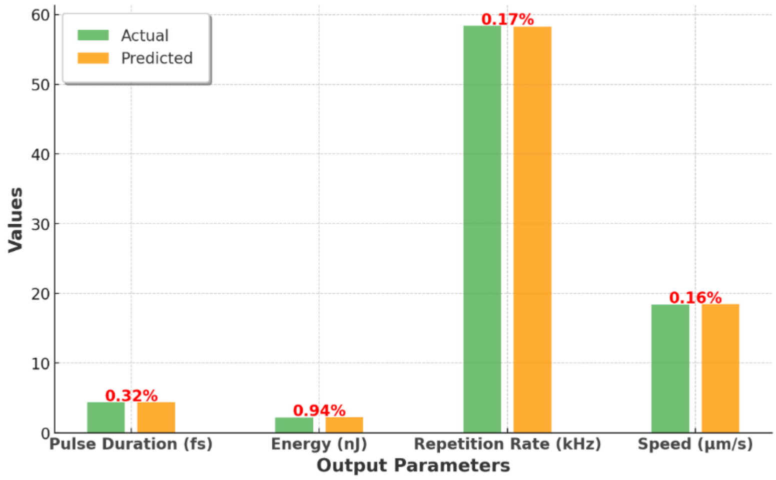

Figure 2: Prediction error % for fluoride sample based on actual and predicted output.

To better evaluate our DNN based simulator, we tested another sample of fluoride material with a different set of parameters. Our simulator estimated a pulse duration of 4.749fs, energy of 7.566nJ, repetition rate of 121.968kHz, and speed of 13.941µm/sec. Predicted numbers were nearly identical to the actual ones, proving our model's remarkable accuracy (see Figure 3). The error margin was exceedingly small, with Pulse Duration deviating by only 0.06%, Pulse Energy by 0.01%, Repetition Rate nearly identical and Speed by 2.52%.

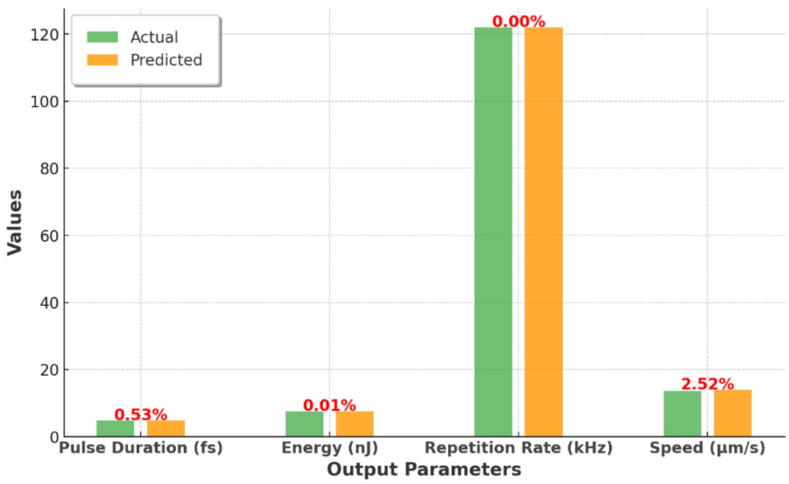

Figure 3: Prediction error % for fluoride sample based on actual and predicted output.

As part of ongoing effort to validate the versatility and precision of DNN-based simulator, a representative sample of germanate material was analyzed, focusing on its unique optical properties and machining requirements. A good correlation between expected and actual results, with slight variances (see Figure 3). The Pulse Duration estimate exhibited an error margin of around 1.03%, while the Pulse

Energy prediction differed by about 1.10%. The Repetition Rate was predicted with a tiny variation of 0.01%, whereas Speed had a little variance of 0.06%. These findings demonstrate the simulator's ability to accurately forecast laser processing parameters for germanateing materials, making it a useful tool for optimizing micromachining procedures.

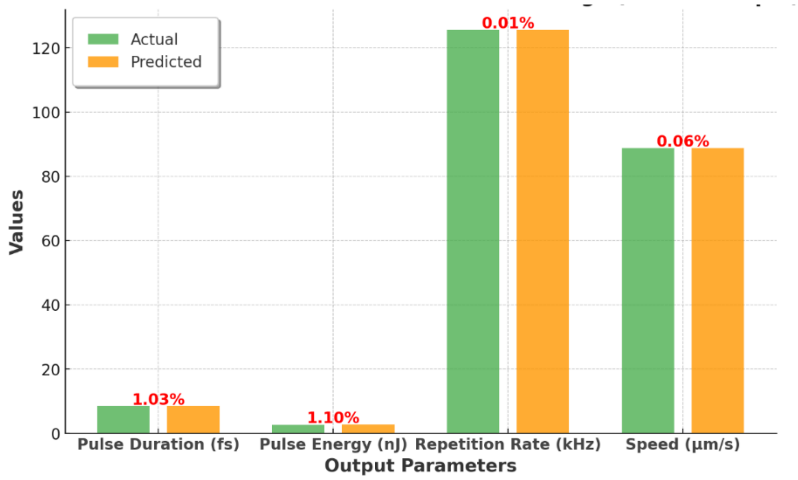

Figure 4: Prediction error % based on actual and predicted output for germanate.

Aiming to further assess the reliability of simulator, another example involving silica material was examined, highlighting its intricate machining characteristics. The study found a difference of around 1.82% in pulse duration and 0.52% in pulse energy (see Figure 5).

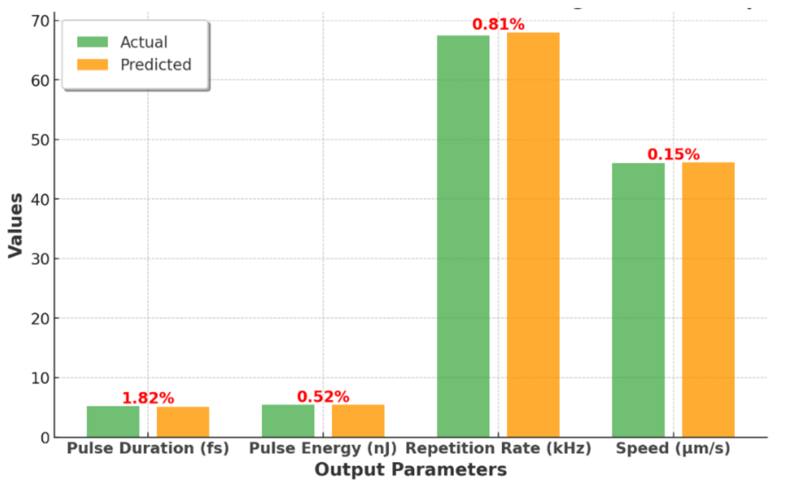

Figure 5: Prediction error % based on actual and predicted output for silicate.

The Repetition Rate prediction varied by 0.81%, but the Speed prediction differed by only 0.15%. These results show that the simulator is highly accurate in forecasting laser micromachining outcomes for silica material, with just slight differences found. This level of precision demonstrates the simulator's efficiency in real-world applications.The simulator created seeks to predict key system performance measurements, how the system performs under various conditions. Simulator's accuracy of 86.61% is remarkable, demonstrating its capacity to accurately forecast laser processing parameters in a variety of difficult situations. The simulator's high degree of precision makes it a priceless tool for streamlining intricate micromachining procedures, opening the door to increased productivity and creativity in industrial settings.

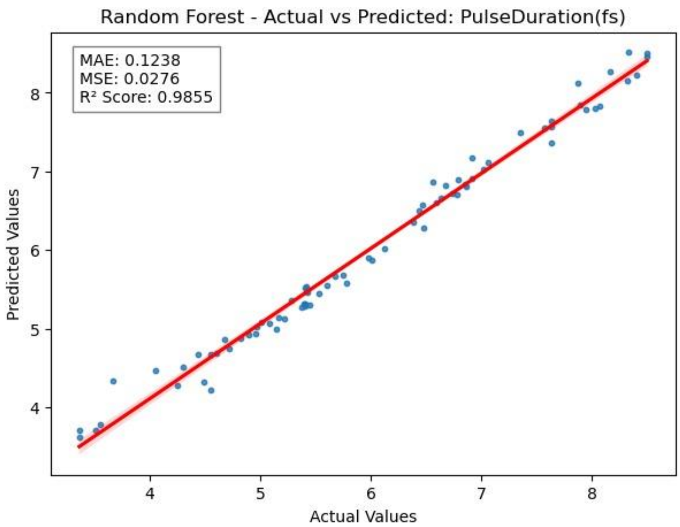

Figure 6: Scatter plots with random forest lines comparing actual vs predicted values for Pulse Duration, illustrating the performance of the model across different parameters

The Random Forest regression model performs exceptionally well in predicting Pulse Duration (fs), as indicated by the R^2 Score of 0.9855. This suggests that the model explains 98.55% of the variance in the actual values, demonstrating a high level of accuracy. The Mean Absolute Error (MAE) of 0.1238 fs and Mean Squared Error (MSE) of 0.0276 indicate minimal deviation between the predicted and actual values (see Figure 6).

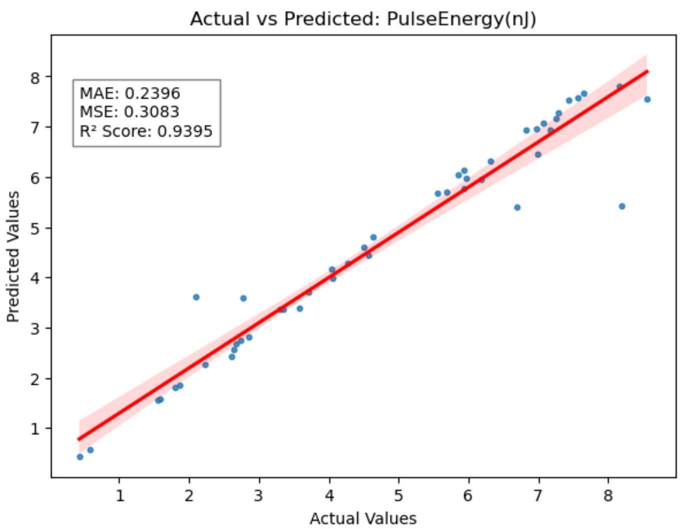

Figure 7: Scatter plots with random forest lines comparing actual vs predicted values for Pulse Energy, illustrating the performance of the model across different parameters.

The Random Forest regression model's performance on predicting Pulse Energy (nJ) appears to be suboptimal. The R^2 Score of 0.9395 suggests that the model explains only about 93.95% of the variance in the actual values, indicating a moderate correlation but significant room for improvement. Additionally, the Mean Absolute Error and Mean Squared Error highlight noticeable deviations between predicted and actual values (see Figure 7).

From the scatter plot, we observe a substantial spread of data points around the red trendline, with many points deviating widely. This suggests that the model struggles with capturing the underlying patterns in the data, leading to inconsistent predictions. The shaded region around the regression line further reflects high variability in the predictions. This performance indicates that Random Forest may not be the best choice for modeling Pulse Energy (nJ), and other regression techniques such as Gradient Boosting or Support Vector Regression should be explored to improve accuracy.

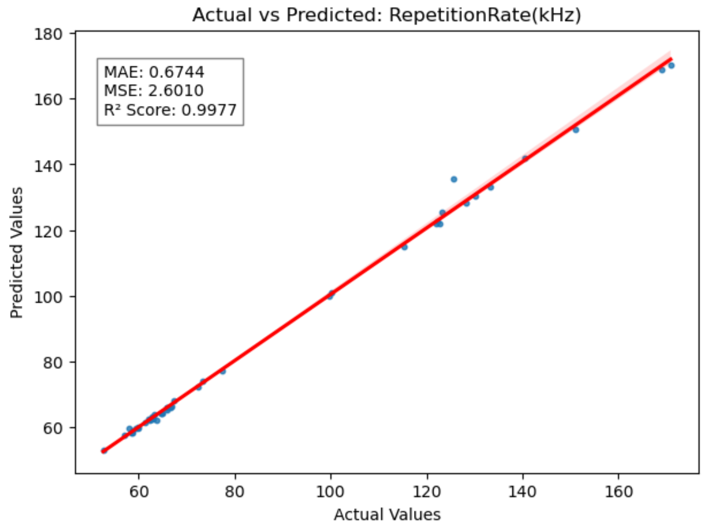

Figure 8: Scatter plots with random forest lines comparing actual vs predicted values for Repetition Rate, illustrating the performance of the model across different parameters.

The performance of the Random Forest regression model for predicting Repetition Rate (kHz) appears to be significantly better compared to its performance on Pulse Energy. The R^2 Score of 0.9977 indicates that the model explains approximately 99.77% of the variance in the actual values, suggesting a strong correlation between predicted and actual values. However, the Mean Absolute Error and the Mean Squared Error indicate that there are still some deviations between the predictions and actual values (see Figure 8). The scatter plot shows that most data points align well with the regression line, although there are some visible outliers, particularly at higher values of Repetition Rate. The shaded confidence interval suggests a relatively low level of uncertainty around the predictions, except at the upper range where variability increases.

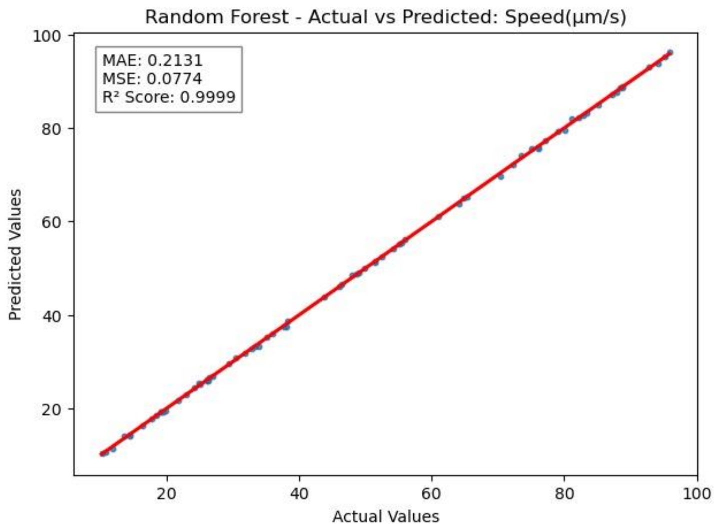

Figure 9: Scatter plots with random forest lines comparing actual vs predicted values for Speed, illustrating the performance of the model across different parameters.

The Random Forest regression model demonstrates exceptional performance in predicting Speed (µm/s). The R^2 Score of 0.9999 indicates an almost perfect fit, meaning that the model explains nearly 100% of the variance in the actual values. Additionally, the Mean Absolute Error (MAE) of 0.2131 µm/s and the Mean Squared Error (MSE) of 0.0774 suggest that the deviations between predicted and actual values are extremely minimal (see Figure 9).

Visually, the scatter plot confirms this outstanding accuracy, as the predicted values align almost perfectly with the actual values along the red regression line. There are no visible outliers or significant deviations, and the confidence interval is nearly nonexistent, indicating a high level of certainty in predictions. Such near-perfect performance suggests that the relationship between input parameters and Speed is highly deterministic, making Random Forest an excellent choice for this particular parameter. However, it is important to ensure that the model is not overfitting by validating its performance on unseen test data.

IV. DISCUSSION

The simulation platform enhances its capabilities by implementing DNN-based research about ultrashort pulse laser micromachining which serves both for parameter optimization during laser processing and simulation functionality. The future development will concentrate on improving the simulator by enhancing simulation capabilities as well as precision levels and extending material applicability and production parameter scope. Researchers need to develop complex modeling approaches with real-time parameter management systems to make the simulator suitable for various processing materials and conditions.Simulation of cumulative pulse interactions stands out as the essential improvement. Continuous development of the DNN-based simulation model indicates the path toward becoming an effective dependable accessible instrument for ultrashort pulse laser micromachining systems. Real-time control enhancement combined with expanded databases makes the simulator accomplish laser machining optimization advancement alongside integrated ensemble learning methods and usability functions. Such developments will create a sophisticated tool which researchers and engineering professionals can use to improve both laser micromachining operations and produce adaptable and precise laser-based manufacturing processes.

V. CONCLUSION

The main purpose of this research was to create a simulator that uses Deep Neural Networks (DNNs) for ultrashort pulse laser micromachining optimization to enhance precision and minimize energy usage. The simulator uses material properties and microchannel dimensions as input variables to predict important parameters including pulse length and repetition rate as well as pulse energy and speed. The application of DNN models enhances laser machining precision and flexibility to an extent which makes them essential for microelectronic and medical equipment industrial applications. The statistical measures selected for model evaluation consisted of MAE, MSE, and R2 which showed the model could effectively predict pulse speed and length. The testing requires further development to expand material variations that include complex substrates including polymers and composites and additional models for cumulative pulse impact analysis. The simulator could be used by a broader range of users through a friendly interface but additional real-time optimizers alongside ensemble learners would elevate its capabilities. Laser micromachining obtains benefits from DNN-based simulators that enhance accuracy together with adaptability and operational efficiency. The enhanced development of this simulator points towards becoming a vital operational instrument for industry-wide laser machining enhancement.

REFERENCES

[1] Rethfeld, B., Ivanov, D. S., Garcia, M. E. & Anisimov, S. I. Modelling ultrafast laser ablation. *J. Phys. D. Appl. Phys.* **50**, (2017).

[2] Khalid, M., Chen, G. Y., Bei, J., Ebendorff-Heidepriem, H. & Lancaster, D. G. Microchip and ultra-fast laser inscribed waveguide lasers in Yb 3+ germanate glass . *Opt. Mater. Express* **9**, 3557 (2019).

[3] Khalid, M. & Arshad, I. Design and Simulation of Photonic Crystal Fibers to evaluate Dispersion and Confinement Loss for Wavelength Division Multiplexing Systems DESIGN AND SIMULATION OF PHOTONIC CRYSTAL FIBERS TO EVALUATE DISPERSION. (2016).

[4] Setia, R. & May, G. S. Modeling and optimization of via formation in dielectrics by laser ablation using neural networks and genetic algorithms. *IEEE Trans. Electron. Packag. Manuf.* **27**, 133–144 (2004).

[5] Shinde, M. . Investigation of Effect of Laser Beam Machining Process Parameters on Performance Characteristics of Stainless Steel. *Res. Technol.* **10**, 621–625 (2017).

[6] Rana, R. S., Chouksey, R., Dhakad & Paliwal. Optimization of process parameter of Laser beam machining of high strength steels: A review. *Today Proc.* **5**, 19191–19199 (2018).

[7] Wadekar, S. & Deokar, S. U. Effect of Process Parameters on Laser Cutting Process: A Review. *Imp. J. Interdiscip. Res.* **2**, (2016).

[8] Khalid, M., Usman, M. & Arshad, I. Germanate glass for laser applications in ∼ 2.1 μm spectral region: A review. *Heliyon* **9**, e13031 (2023).

[9] Rajesh, A. S., Prabhuswamy, M. S. & Krishnasamy, S. Smart Manufacturing through Machine Learning: A Review, Perspective, and Future Directions to the Machining Industry. *J. Eng. (United Kingdom)* **2022**, (2022).

[10] Bundesanstalt, G. Issue " Advanced Machining Technology ". (2023).

[11] Jiang, J. A survey of machine learning in additive manufacturing technologies. *Int. J. Comput. Integr. Manuf.* **00**, 1–23 (2023).

[12] McDonnell, M. D. T. *et al.* Machine learning for multi-dimensional optimisation and predictive visualisation of laser machining. *J. Intell. Manuf.* **32**, 1471–1483 (2021).

[13] Patidar, D. & Rana, R. S. The effect of CO2 laser cutting parameter on Mechanical & Microstructural characteristics of high strength steel-a review. *Mater. Today Proc.* **5**, 17753–17762 (2018).

[14] Tani, S. & Kobayashi, Y. Ultrafast laser ablation simulator using deep neural networks. *Sci. Rep.* **12**, 1–8 (2022).

[15] Holder, D. *et al.* Analytical model for the depth progress of percussion drilling with ultrashort laser pulses. *Appl. Phys. A Mater. Sci. Process.* **127**, 1–8 (2021).

[16] Kotadiya, D. J., Kapopara, J. M., Patel, C. G. & Pandya, D. H. Parametric analysis of process parameter for Laser cutting process. *Mater. Today Proc.* **5**, 5384–5390 (2018).

[17] Khalid, M., Chen, G. Y., Ebendorff-Heidepreim, H. & Lancaster, D. G. Femtosecond laser induced low propagation loss waveguides in a lead-germanate glass for efficient lasing in near to mid-IR. *Sci. Rep.* **11**, 1–12 (2021).

[18] Kobayashi, Y. et al. Fully Automated Data Acquisition for Laser Production Cyber-Physical System. IEEE J. Sel. Top. Quantum Electron. 27,1–8 (2021).